



A Set of Methods to Predict Water Inrush from an Ordovician Karst Aquifer: A Case Study from the Chengzhuang Mine, China

Hao Li^{1,2} · Haibo Bai² · Jianjun Wu³ · Qingbin Meng² · Kai Ma² · Luyuan Wu² · Fanfei Meng² · Shaojie Wang⁴

Received: 4 April 2017 / Accepted: 22 December 2018 / Published online: 3 January 2019
© Springer-Verlag GmbH Germany, part of Springer Nature 2019

Abstract

To ensure safe mining of the 3153 working face in the Chengzhuang mine, with its thin aquifuge, we developed a complete set of methods, including transient electromagnetics, drilling, a water injection experiment, and a numerical simulation based on a new constitutive model. Thus, the groundwater distribution, the aquifuge thickness, and the floor damage thickness were obtained successively and the results from each method could be mutually verified. The main results were: (1) The floor damage thickness decreases when the backfill affects the floor, and further thickens as the hanging roof area increases. (2) Under cyclic loading, tension and compression damage zones are connected. The deepest compression damage lags the coal wall, while the point of maximum tensile damage lags the deepest compression damage zone, thus forming an inclined water-conductive zone.

Keywords Groundwater inrush · Floor damage thickness · Transient electromagnetic method · Water injection experiment · Numerical Simulation

Introduction

In China, more than 1300 water inrush incidents from coal seam floors have occurred during the past 60 years, leading to significant economic losses and casualties (Wu et al. 2013). The Carboniferous-Permian coal-bearing strata in north China directly overlay the Ordovician karst aquifer (Li et al. 2015), and the thickness of the aquifuge between

the coal seam and Ordovician limestone aquifer is usually 30–60 m or even thinner (Lu and Wang 2015).

Theoretical and numerical models, physical analogs, and in-situ tests have been used to prevent such disasters. Zhu et al. (2008b) obtained an analytical solution to the stress in the floor using an elasticity model, and verified the results using the “strain method”. Zhang et al. (2016) used the similar simulation test method to obtain the fracture thickness of the mine floor. Zhu et al. (2008a) and Zhu and Wei (2011), using the ideal elastic-brittle constitutive model, obtained the damaged thickness of the coal seam floor by numerical simulation, based on the premise that damage will occur when the stress in the rock exceeds the strength limit.

However, these studies generally used a single or unreasonable combination of methods to forecast the stress, strain, displacement, and plastic zone of the floor rock. In fact, the nature of water-bursting from the Ordovician limestone aquifer is that the combined action of mining and the confining water pressure will cause micro-crack initiation, expansion, and penetration of the rock, which in turn causes the floor to fail, from top to bottom. When the aquifuge can no longer withstand the pressures, a disaster will occur. Therefore, we need to use reasonable measures to study the thickness of the damage (Guo et al. 2009). In addition, as a necessary condition for predicting a water inrush, it is essential to

Electronic supplementary material The online version of this article (<https://doi.org/10.1007/s10230-018-00572-3>) contains supplementary material, which is available to authorized users.

✉ Haibo Bai
hbbaicumtedu@126.com

- ¹ Key Laboratory of In-situ Property-improving Mining of Ministry of Education, Taiyuan University of Technology, Taiyuan 030024, Shanxi, China
- ² State Key Laboratory for Geomechanics and Deep Underground Engineering, China University of Mining and Technology, Xuzhou 221116, Jiangsu, China
- ³ Shanxi China Coal Huajin Energy Limited Liability Company, Hejin 043300, Shanxi, China
- ⁴ Civil Engineering College, Tianjin Chengjian University, Tianjin 300384, China

understand the groundwater distribution and aquifuge thickness. Based on the above analysis, a complete set of methods have been developed: first, the distribution of the Ordovician groundwater is detected using the transient electromagnetic method (TEM); then, on this basis, instead of using the “strain method”, we used a water injection experiment (WIE) to test the floor damage thickness at different depths; then a new constitutive model, which is consistent with the engineering practice, was developed, which allowed us to obtain the floor damage thickness by numerical simulation.

The Study Area and Mining Plan

The Chengzhuang mine is located northwest of Jincheng, Shanxi province (Fig. 1s). The strata in the area, from top to bottom, consists of four aquifer groups and two aquifuge groups (Fig. 1). The former includes the: Quaternary loose media aquifer group, Permian sandstone aquifer group, and the Carboniferous and Ordovician carbonate karst aquifer group. The last includes the Permian sandstone and Carboniferous mudstone aquifuge groups. There are numbers of aquifer groups in the roof but, so far, water inrush from the roof has not occurred, because there is less water in the first three aquifers, and the aquifuge thickness between these aquifers and the working face is large. In contrast, the distance

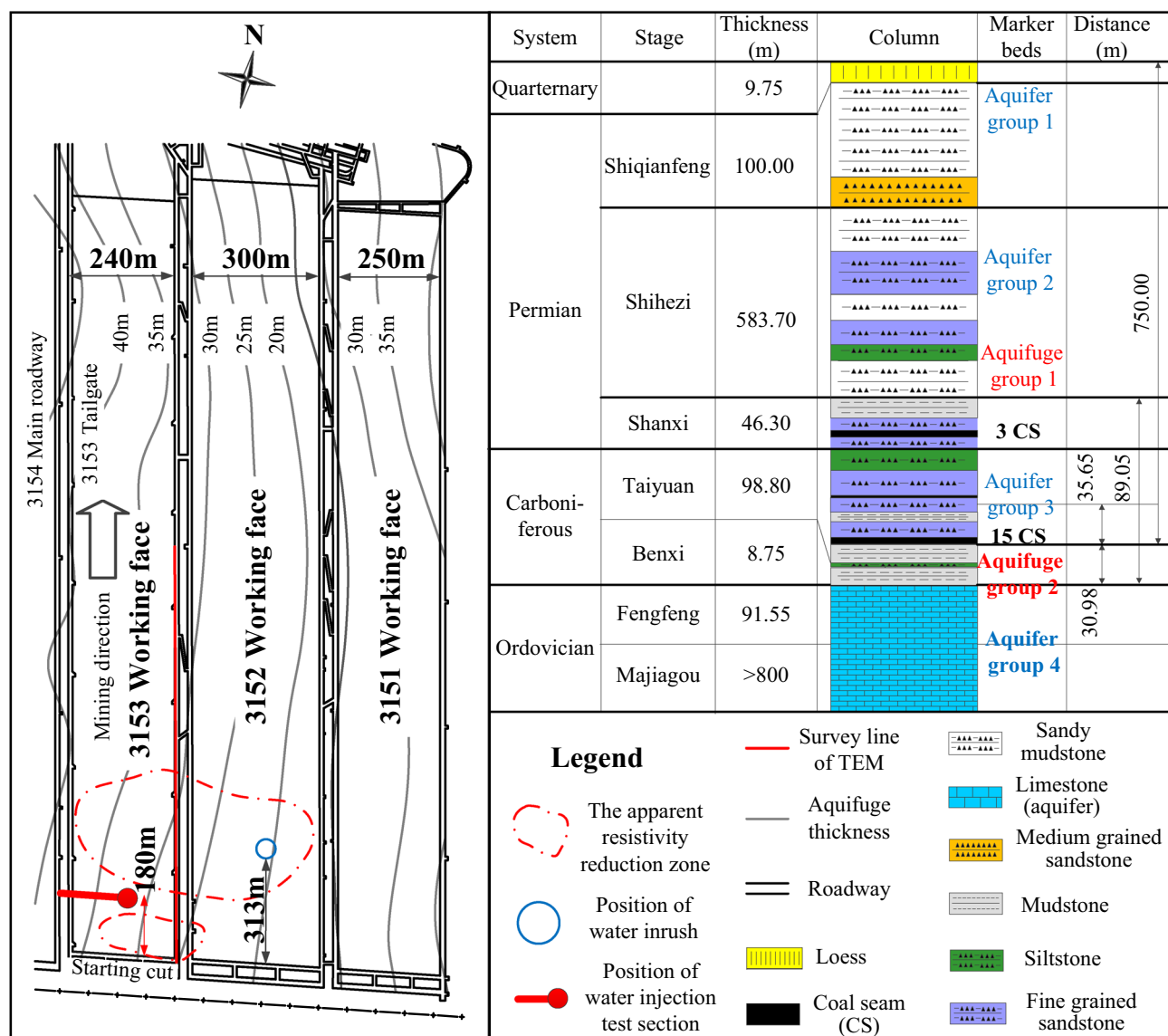


Fig. 1 The arrangement and stratigraphic column of the 3153 working face

between the #15 coal seam and Ordovician confined aquifer is very small; in particular, the aquifuge thickness of the 3152 working floor is only 20 m, which resulted in a flooding disaster on Nov. 6, 2014 (Fig. 1). The main reasons for this were because: (1) the immediate roof in the working face is a fine sandstone stratum with a thickness of 12 m, thus, the distance of initial caving is 60 m. Given the increased hanging roof area, the rock pressure on the floor became greater and greater; and (2) the engineers did not detail the geological and hydrogeological conditions of the 3152 working face. The mining plan was unreasonable because the hanging roof area and working face length were uncontrolled.

To prevent future flooding disasters, we compared the design of working faces in adjacent coal mines and the empirical formula of the floor damage thickness (Feng et al. 2010) with the engineering practice of the 3153 working face. A mining plan with a face length of 240 m and an initial collapse distance of 44 m was designed. Next, the floor damage thickness for this mining plan was verified using the “complete methods” discussed in this paper.

Figure 1 will be placed near here during the printing process.

In-Situ Tests

In order to avoid water inrush accidents during the mining of the 3153 working face, we used a variety of in-situ monitoring methods.

Transient Electromagnetic Method (TEM)

If there is no groundwater or if the aquifer is far from the coal seam, there is no need to test the floor damage thickness. Therefore, the TEM used. The basic principle of the TEM is that a pulsed primary magnetic field is sent into the floor; the magnetic field induces an electric current in

the rock, which propagates to the surroundings at different speeds due to the resistivity of the different media. When the current encounters an aquifer, a secondary magnetic field forms around it, and we can get the groundwater distribution by measuring this electromagnetic signal (Hu et al. 2014).

Using the TEM along the tailgate of the 3153 working face showed the presence of two areas with high water capacity in the Ordovician limestone (Fig. 2), where the apparent resistivity was relatively low. Both were located within 510 m from the starting cut, and the vertical distance from the coal seam was about 30 m. Water inrush happened in the working face in the apparent resistivity reduction area (Fig. 1); therefore, it was important to understand the groundwater distribution.

Figure 2 will be placed near here during the printing process.

Drilling Data

Drilling data is important for determining the aquifer water pressure, thickness of the aquifuge, and lithology. The results of the first two were easy to get; the Ordovician limestone water pressure was about 2 MPa and the aquifuge for the working face was about 30 m thick. This is a relatively thin aquifuge. Therefore, a cement slurry should be injected into the limestone stratum to ensure mining safety. However, the drilling data showed that dolomite occurred 180 m from the starting cut.

Therefore, at a distance of 180 m from the starting cut, rock samples at different depths (755, 775, 795, and 815 m) from the top of the Ordovician were taken for microscopic examination. The results showed that the rock at the top of the Ordovician strata was dolomite, which has a low permeability coefficient (Fig. 3). This meant that the floor water inflow is small in this area and that it would be safe to conduct a water injection experiment there.

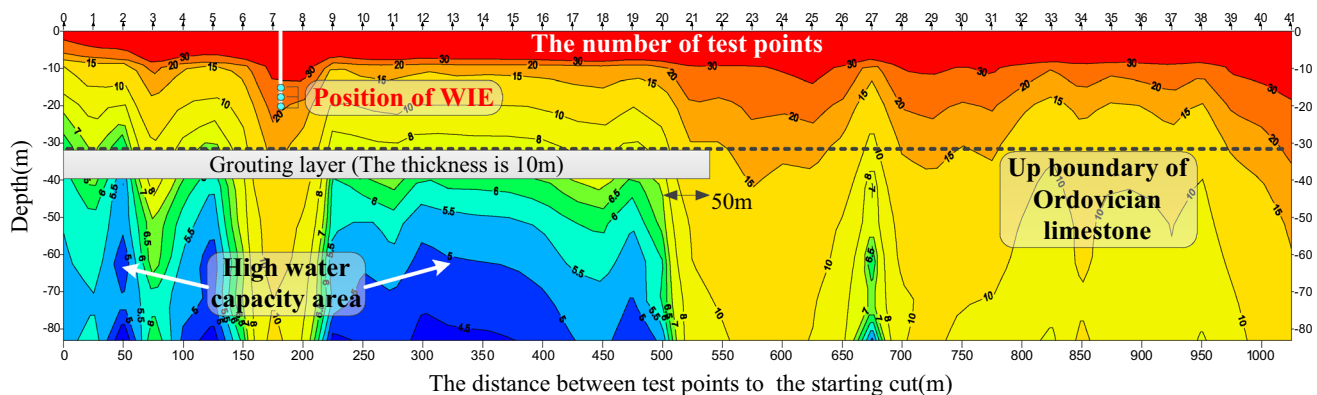


Fig. 2 The apparent resistivity in 3153 working face floor

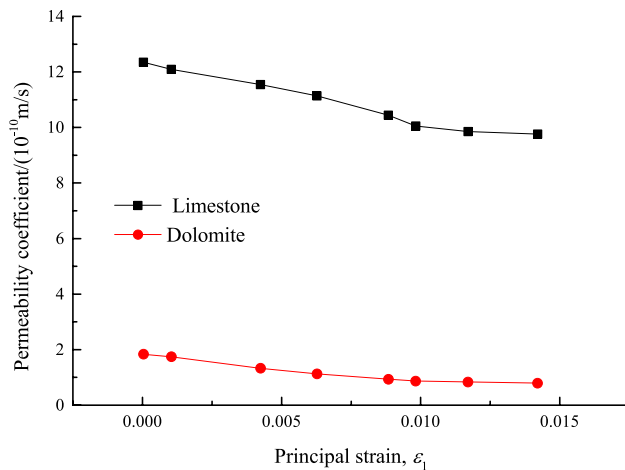


Fig. 3 Comparison of permeability coefficient between dolomite and limestone (in elastic deformation stage)

Figure 3 will be placed near here during the printing process.

Water Injection Experiment (WIE)

The mine's engineers grouted the top of the Ordovician strata (Fig. 2), as discussed above, which ensured that a water inrush disaster would not occur before or during the

WIE. Although the grouting might have caused errors in the WIE, it was judged necessary.

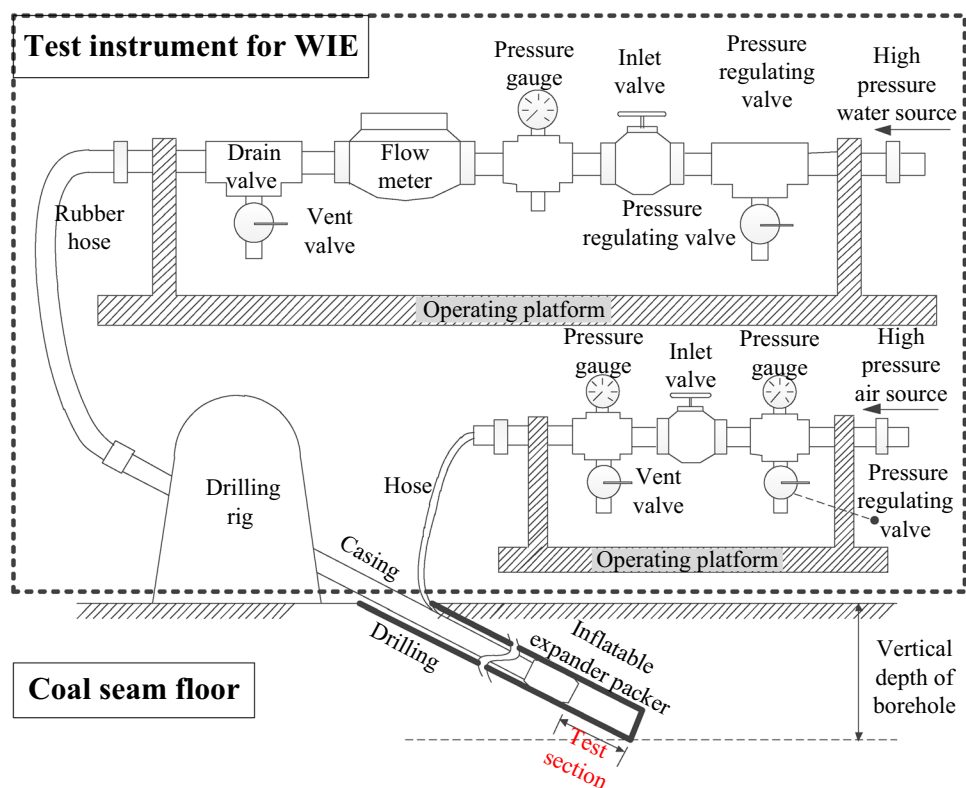
The purpose of a WIE is to determine the damaged thickness of the mine floor. The principle of a WIE is simple; that is, coal excavation causes different damage and permeability at different depths of the floor rock. Thus, a higher average flow, Q , means more serious damage to the borehole (Li et al. 2016b).

Given the TEM results and the potential influence of the WIE on installation of equipment near the working face, the observation point was arranged 180 m from the starting cut, in the 3154 main roadway (Fig. 1). We used a set of instruments for WIE (Fig. 4), and three testing depths, i.e. 16, 18, and 20 m (Fig. 5). The drilling parameters are shown in Table 1.

Figures 4 and 5 and Table 1 will be placed near here during the printing process.

WIE began in early July 2015 and ended in mid-August 2015. During the mining process, Q data were recorded every 10 m of advancing distance. The results (Fig. 6) showed that when the mining face was 20 m from the test section, the damage thickness was less than 16 m; however, when the distance between the mining face and the test section was less than 7 m, the damage thickness suddenly increased to ≈ 18 –20 m. The maximum hanging roof area occurred when the mining face had passed the test section by ≈ 7 m, which was when the Q value reached its first peak

Fig. 4 The instruments for WIE



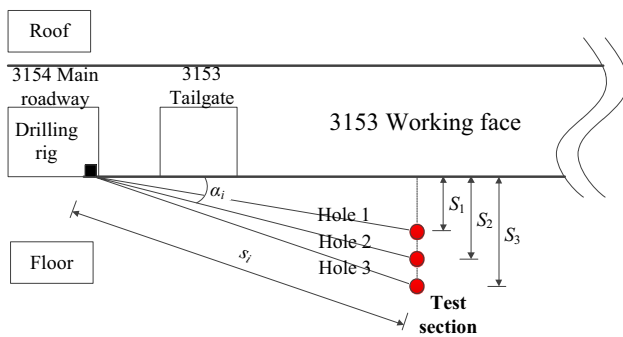


Fig. 5 Position of WIE (Profile)

Table 1 The parameters of drilling hole for floor damage thickness

Number	Borehole diameter (mm)	Azimuth	α	s_i (m)	S_i (m)
1	89	306°11'	23°12'	40.62	16
2		276°57'	24°21'	43.66	18
3		291°29'	25°24'	46.63	20

α is the inclination angle of drilling, s_i is the length of holes, S_i is the maximum vertical depth of holes (Fig. 7)

(1.86 L/h, $S_1 = 16$ m). The average flow was 0 L/h in hole 3 (Fig. 6); however, the flow slightly increased when the distance between the mining face and test section was 7 m, which means that the floor damage lags the mining face and deepens again. Based on these findings, we judged the maximum damage thickness as less than 20 m in the mining process. As a result of periodic roof caving, the Q value decreased when the mining face passed the test section by 19 and 34 m; at the latter point, the value of Q reached a second peak (2.02 L/h, $S_1 = 16$ m) due to the increased amount of hanging roof area, which means that the degree of floor damage increased again in the mined-out area. The value of Q stabilized at 1.42 L/h, until the mining face passed the test section by 57 m. In short, the hanging roof area greatly affects the amount of floor damage, so that the position of maximum damage thickness lags the mining process.

Figure 6 will be placed near here during the printing process.

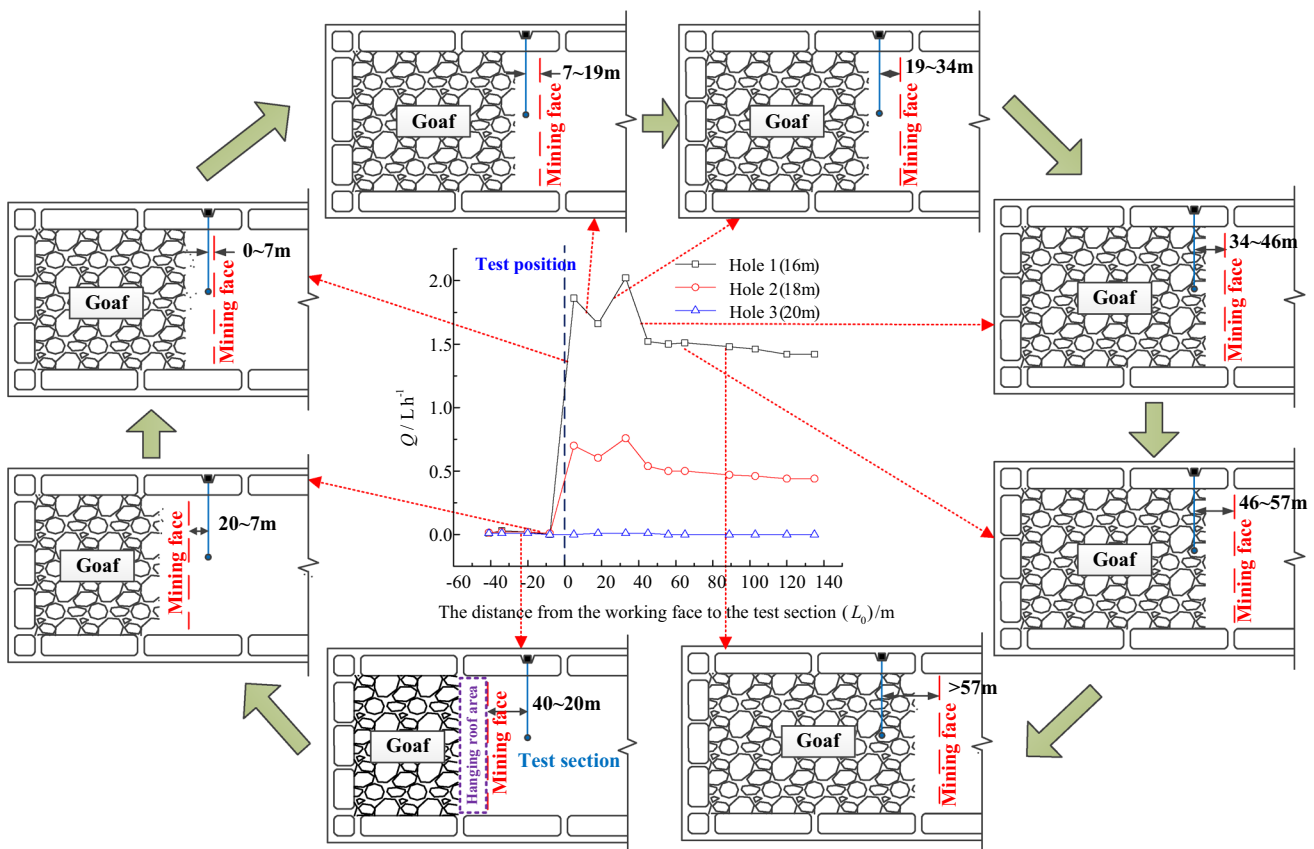


Fig. 6 Average flow curves of three holes with different L_0 (L_0 is the distance between the mining face and the test points of WIE)

Numerical Simulation

Numerical simulation results can be quite different with different constitutive models. To calculate the thickness of the damaged portion of the aquifuge, it was essential to establish a constitutive model that conforms to the mining engineering.

Constitutive Model

A constitutive model, named the D-P elastoplastic damage model, was developed. It reflects the mechanical properties of rock materials during cyclic loading and unloading (Fig. 7), such as occurs during coal mining, better than a conventional constitutive model (e.g. Li et al. 2016a; Ou et al. 2013). The expressions are shown in Eqs. (1) to (4). In the effective stress space, the expression described by the hydrostatic stress \bar{p} and the deviatoric stress \bar{q} (Lee and Fenves 1998; Lubliner et al. 1989) is:

$$F = [\bar{q} - 3\alpha\bar{p} + \beta\langle\bar{\sigma}_{i\max}\rangle - \gamma\langle-\bar{\sigma}_{i\max}\rangle]/(1-\alpha) - \sigma_c = 0 \quad (1)$$

where $\alpha = [(\sigma_{b0}/\sigma_{c0}) - 1]/[2(\sigma_{b0}/\sigma_{c0}) - 1]$, $\beta = \bar{\sigma}_c/\bar{\sigma}_t(1-\alpha) - (1+\alpha)$, $\gamma = 3(1-K_c)/(2K_c-1)$, $\bar{\sigma}_{i\max}$ ($i=1, 2, 3$) is the maximum principal effective stress; σ_{b0}/σ_{c0} is the ratio of initial equibiaxial compressive yield stress to initial uniaxial compressive yield stress; K_c is the ratio of the second stress invariant on the tensile meridian to that on the compressive meridian; and $\bar{\sigma}_c$, $\bar{\sigma}_t$ are the effective tensile stress and the effective compressive stress,

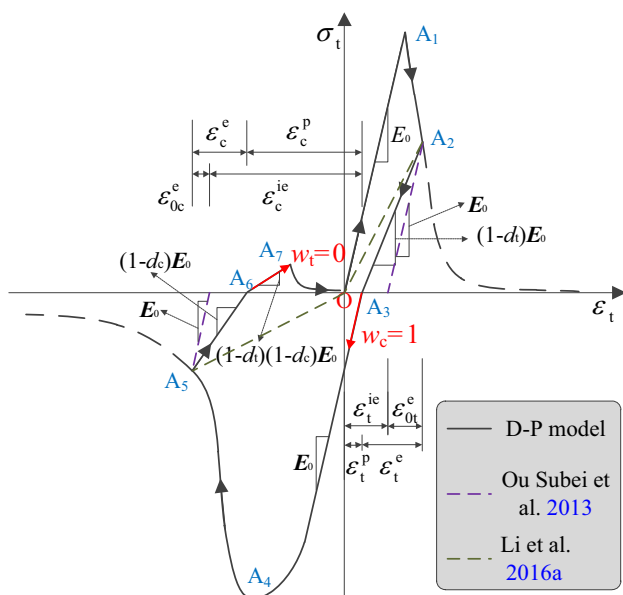


Fig. 7 Changes of mechanical properties during cyclic loading and unloading

respectively. The plastic potential function described by \bar{p} and \bar{q} is:

$$G = \sqrt{(\delta\sigma_{t0} \tan \psi)^2 + \bar{q}^2} - \bar{p} \tan \psi \quad (2)$$

where δ is eccentricity, that defines the rate at which the function approaches the asymptote; σ_{t0} is the uniaxial tensile stress at failure; and ψ is the dilation angle measured in the p - q plane at high confining pressure. The relationship between stress and strain during cyclic loading and unloading is shown in Eq. 3:

$$\sigma = (1-d)D_0^e(\epsilon - \epsilon^p) \quad (3)$$

where σ is the stress vector; D_0^e is the undamaged elastic stiffness matrix; ϵ is the total strain vector; ϵ^p is the plastic strain vector; d is determined by the stress state and the uniaxial damage variables (i.e. d_t and d_c). The relationship between them is: $1-d = (1-s_t d_c)(1-s_c d_t)$; s_t and s_c are the function of stress, and $s_t = 1 - \omega_t r(\sigma_i)$, $s_c = 1 - \omega_c [1 - r(\sigma_i)]$, $0 \leq \omega_t, \omega_c \leq 1$, $i=1, 2, 3$; σ_i ($i=1, 2, 3$) are the principal stress components; $r(\sigma_i) = \sum_{i=1}^3 \langle \sigma_i \rangle / \sum_{i=1}^3 |\sigma_i|$, $\langle \sigma_i \rangle = (|\sigma_i| + \sigma_i)/2$; and ω_t and ω_c are weight factors (Fig. 7).

Figure 7 will be placed near here during the printing process.

According to the geometric relationship shown in Fig. 4, the relationship between ϵ_t^p and d_t , and ϵ_c^p and d_c can be deduced, as shown in Eqs. 4a and 4b, respectively.

$$\epsilon_t^p = \epsilon_t^{ie} - d_t \sigma_t / [(1-d_t)E_0] \quad (4a)$$

$$\epsilon_c^p = \epsilon_c^{ie} - d_c \sigma_c / [(1-d_c)E_0] \quad (4b)$$

where $\epsilon_t^{ie} = \epsilon_t - \epsilon_{0t}^e = \epsilon_t - \sigma_t/E_0$ and $\epsilon_c^{ie} = \epsilon_c - \epsilon_{0c}^e = \epsilon_c - \sigma_c/E_0$. The numerical simulation process based on the above equations is shown in Fig. 8.

Figure 8 will be placed near here during the printing process.

Numerical Model and Parameters

As shown in Fig. 1, the mining depth of the 3153 working face is of approximately 750 m, without obvious faults, karst collapse columns, or other geological structures. According to the drilling data, the water pressure of the Ordovician confined aquifer is 2 MPa.

Based on the mine's geological conditions, a plane strain numerical model 200 m long and 200 m high was established in the finite element software ABAQUS (Fig. 9). Vertical and horizontal displacement constraints were applied to the bottom and left and right boundaries of the numerical model, respectively, and a vertical downward pressure of 16.14 MPa was applied to the upper boundary to simulate the overlying rock mass with a unit

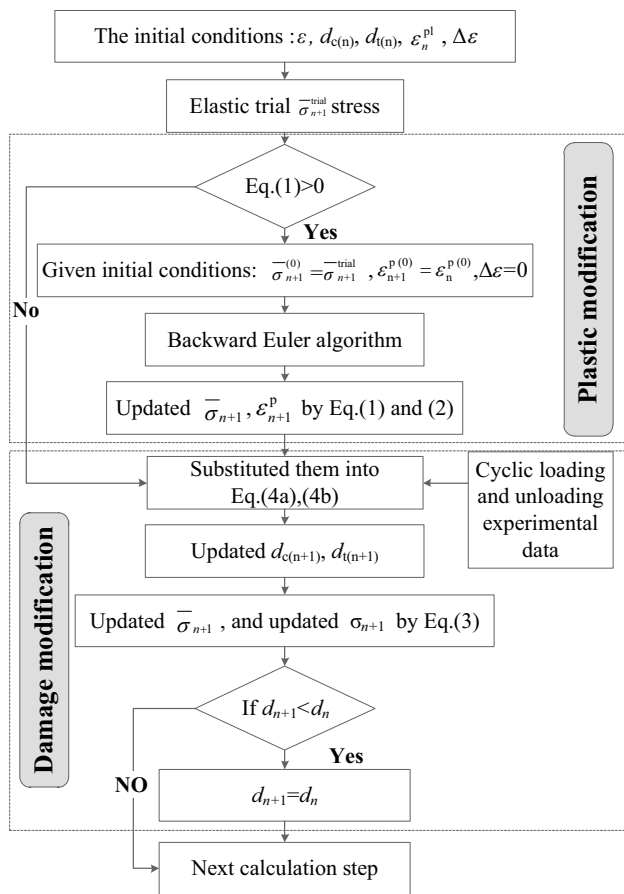


Fig. 8 Numerical calculation process

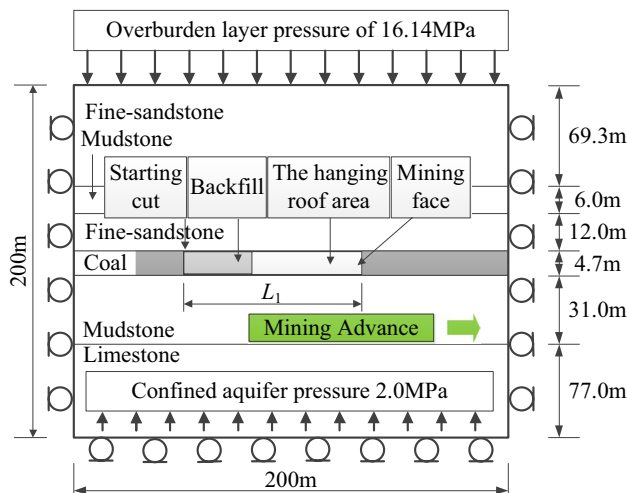


Fig. 9 Numerical calculation model

weight of 2500 KN/m³ and a thickness of 645 m. A vertical upward pressure of 2 MPa was applied to the bottom boundary to simulate the aquifer's water pressure. During

extraction, the goaf area was filled with a soft elastic material to approximately simulate the support capacity of the fallen roof rock. A 22 m long filling body was added after the first roof caving of 44 m, and an 8 m long backfill was continuously added after periodic caving. Young's modulus for this material was set at 470 MPa; the Poisson's ratio was 0.25 (Cheng et al. 2010).

Figure 9 will be placed near here during the printing process.

The rock parameters can be obtained by cyclic loading and unloading experiments; the results are shown in Table 2 and Fig. 10.

Table 2 and Fig. 10 will be placed near here during the printing process.

Numerical Simulation Results

The numerical simulation results before the initial caving (i.e. $L_1 = 36, 40$, and 44 m) and after periodic caving (i.e. $L_1 = 48, 52$, and 72 m) are compared with the results of WIE (Fig. 11).

Figure 11 will be placed near here during the printing process.

1. During the mining process, the floor rock undergoes the cyclic loading of compression—tension—compression. Stress concentrates at the front of the mining face and a shear zone is formed. A stress relief zone forms in the goaf, as the confining pressure drops to zero. With the collapse of the roof and the compaction of the filling body, the stress in the floor increases again.
2. As mining advances, the damaged floor thickness strongly depends on the mining operation. Before the initial caving ($L_1 \leq 40$ m), the thickness increased linearly, from $l_1 = 0$ m to $l_1 = 17.6$ m; with the increase of hanging roof area, the increment was ≈ 1.0 to 2.4 m. When $L_1 = 44$ m, the roof caved for the first time and the thickness increased slightly, to 18 m. During the periodic caving, the thickness at the mining face increased with the increase of the hanging roof area (i.e. $L_1 = 48$ m), but then decreased due to the influence of the backfill (i.e. $L_1 = 52$ m). Floor damage thickness fluctuated and finally stabilizes at about 18.5 m ($L_1 = 72$ m), which is obviously less than the aquifuge thickness of 30 m, which means that the mining plan is safe.
3. Tensile damage further enhances permeability. First, compressive damage occurs in the stress concentration zone, and then tensile damage occurs in the stress relief zone, resulting in a sharp increase in permeability (Zhang and Xiao 2008). The position of maximum tensile damage is $\approx l_4 = 7.5$ m, lagging behind the coal wall, while the deepest compression damage lagged the coal wall by 2 to 5 m, thus forming an inclined, water-conducting channel.

Table 2 Parameters of numerical simulation

	ρ (kg/m ³)	E_0 (GPa)	μ	ψ	δ	σ_{b0}/σ_{c0}	K
Coal	1600	3.60	0.3	14	0.1	1.16	0.667
Mudstone	2500	3.53	0.25	15	0.1	1.16	0.667
Backfill	2000	0.47	0.25	–	–	–	–
Fine sandstone	2500	13.1	0.20	18	0.1	1.16	0.667
Limestone	2600	10.8	0.22	17	0.1	1.16	0.667

ρ is the density of materials, E_0 is the initial elastic modulus, μ is the Poisson's ratio, ψ is the dilatancy angle, δ is a parameter to determine the curvature of yield surface in tensile section, σ_{b0}/σ_{c0} is the ratio of equivalent biaxial compression yield stress to the uniaxial compression yield stress, K is a parameter to control the shape of the yield surface in the π plane

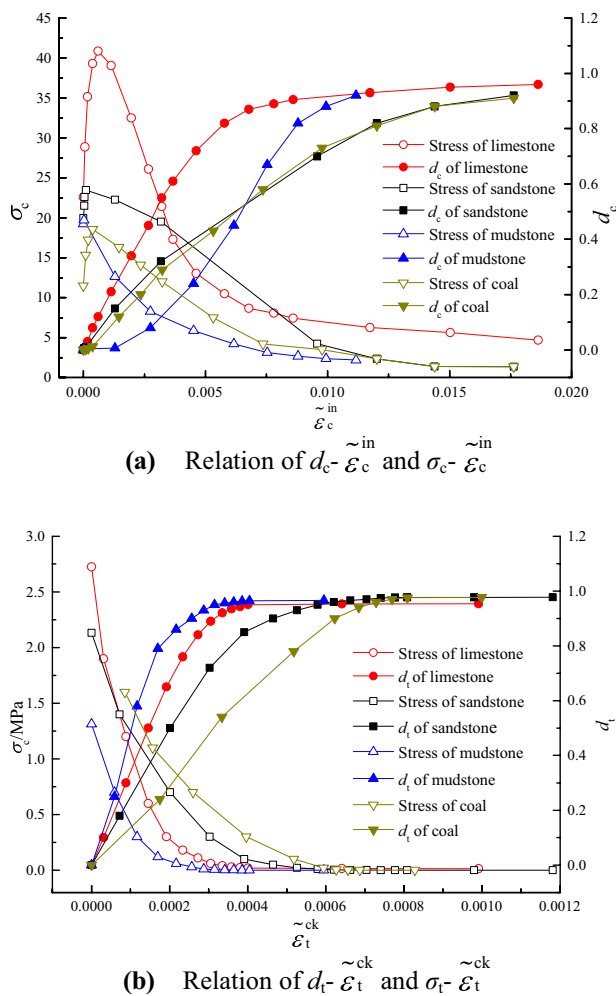


Fig. 10 Damage evolution curves of limestone, sandstone, mudstone, and coal. **a** Relation of $d_c - \tilde{\epsilon}_c^{in}$ and $\sigma_c - \tilde{\epsilon}_c^{in}$. **b** Relation of $d_t - \tilde{\epsilon}_t^{ck}$ and $\sigma_t - \tilde{\epsilon}_t^{ck}$

Discussion

The set of methods to predict a water inrush in mines where the mine floor is a thin aquifuge is illustrated in Fig. 12. First, the groundwater distribution is obtained by

TEM; ignoring this hydrogeological data can have catastrophic consequences (Yin and Zhang 2005). Second, the lithology, confined water pressure, and aquifuge thickness is obtained from the drilling data. Third, the WIE is used to test the thickness of damaged floor, which determines whether or not an inrush will occur. Four, unlike elastic theory (Zhu et al. 2008a), elastoplastic theory (Zhang et al. 2016), or elastic damage (Zhu and Wei 2011), the D-P elastoplastic damage model can reflect the mechanical properties of the rock floor as mining advances (Fig. 8). Results, such as how the maximum damage lags the coal wall and deepens again as the hanging roof area increases, can be obtained. The conclusion agreed with the WIE results.

Figure 12 will be placed near here during the printing process.

Conclusions

A complete set of methods has been developed to obtain the groundwater distribution and the thickness of the aquifuge, especially the thickness of the mine floor damage. This provides the basis for preventing a water inrush from the Ordovician limestone aquifer. Its effectiveness was demonstrated at the 3153 working face of the Chengzhuang mine. The main conclusions are summarized as follows:

1. TEM and borehole data can be used to obtain groundwater distribution and confined water pressure, respectively. In addition, the two methods verified the aquifuge thickness of 3153 working face to be about 30 m. Similarly, the damage thickness of the working face (≈ 18.5 m) was obtained by combining the results of the WIE and numerical simulations.
2. The thickness of the floor damage is determined by compression, which strongly depends on the amount of backfill and roof hanging area. The thickness at the coal wall decreases as the backfill affects the floor. Although the hanging roof area increases damage at the coal wall, the

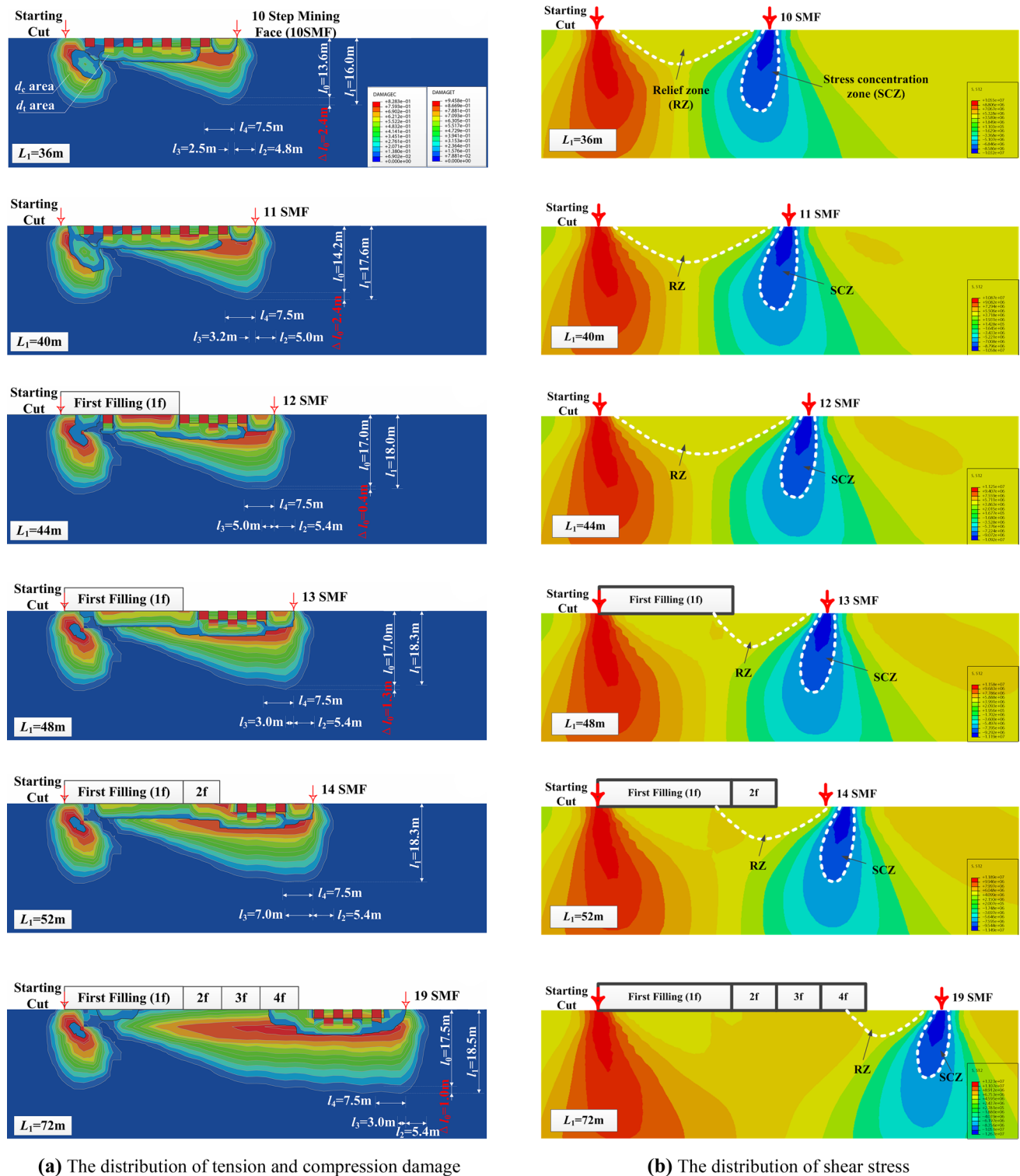


Fig. 11 The numerical simulation results. **a** The distribution of tension and compression damage. **b** The distribution of shear stress

increment of the thickness gradually decreases during backfill compaction. The floor damage thickness thus fluctuates, but finally stabilizes.

- As mining proceeds, compressive damage occurs first, followed by tensile damage, and the water resistance of the rock floor seriously deteriorates unless it is grouted.

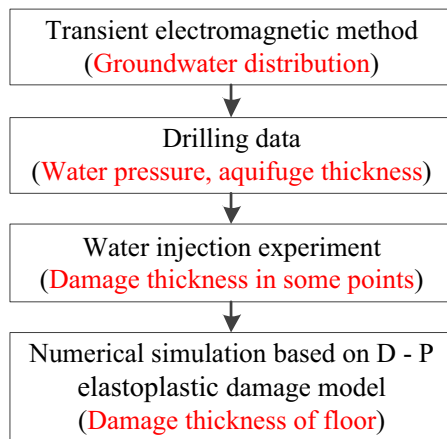


Fig. 12 The steps to prevent the water inrush from floor

The deepest compressive damage lags the coal wall, while the position of maximum tensile damage lags the deepest compressive damage zone, which causes water inrush events to lag the coal wall. This result is consistent with that of the WIE.

Acknowledgements The authors sincerely thank Mr. Wang Qiang at Southeast University for providing work stations and related data access. This work was supported by the Research Innovation Program for College Graduates of Jiangsu Province (KYLX16_0537) and the National Natural Science Foundation of China (51704280). We also thank the anonymous referees for their careful reading of this article and valuable suggestions.

References

- Cheng YM, Wang JA, Xie GX, Wei WB (2010) Three-dimensional analysis of coal barrier pillars in tailgate area adjacent to the fully mechanized top caving mining face. *Int J Rock Mech Min Sci* 47:1372–1383
- Feng MM, Mao XB, Zhu QH (2010) Effect of lithologic association of the water-resisting strata in coal seam floor on water insulating. *J Min Safe Eng* 27:404–409 (in Chinese and abstract in English)
- Guo H, Adhikary DP, Craig MS (2009) Simulation of mine water inflow and gas emission during longwall mining. *Rock Mech Rock Eng* 42:25–51
- Hu XW, Zhang PS, Yan JP, Guo LQ (2014) Improvement of means for interpretation of advanced water detection of tunnels by transient electromagnetic method. *Chin J Geotech Eng* 36:654–661 (in Chinese and abstract in English)
- Lee J, Fenves GL (1998) Plastic-damage model for cyclic loading of concrete structures. *J Eng Mech* 124:892–900
- Li L, Zhou Z, Li S, Xue Y, Xu Z, Shi S (2015) An attribute synthetic valuation system for risk assessment of floor water inrush in coal mines. *Mine Water Environ* 34:288–294
- Li Z, Feng G, Zhai C (2016a) Study on “triangle” water-inrush mode of strong water-guide collapse column. *J Cent South U* 23:2402–2409
- Li HL, Bai HB, Ma D, Xu J, Qian HW, Tian CD (2016b) Experimental study on mining-induced failure depth lagging coal wall secondary deepening rule. *J Min Safe Eng* 33:318–323 (in Chinese and abstract in English)
- Lu YL, Wang LG (2015) Numerical simulation of mining-induced fracture evolution and water flow in coal seam floor above a confined aquifer. *Comp Geo* 67:157–171
- Lubliner J, Oliver J, Oller S, Onate E (1989) A plastic-damage model for concrete. *Int J Solids Struct* 25:299–326
- Ou S, Wang L, Wang P (2013) Numerical analysis of seepage flow characteristic of collapse column under the influence of mining. *Int J Min Sci Technol* 23:237–244
- Wu Q, Fan S, Zhou W, Liu S (2013) Application of the analytic hierarchy process to assessment of water inrush: a case study for the no. 17 coal seam in the Sanhejian Coal Mine, China. *Mine Water Environ* 32:229–238
- Yin SX, Zhang J (2005) Impacts of karst paleo-sinkholes on mining and environment in northern China. *Environ Geol* 48(8):1077–1083
- Zhang HW, Xiao M, Fan GB (2008) Stress-damage-seepage coupling analysis of surrounding rock of large-scale underground caverns. *Rock Soil Mech* 29:1813–1818 (in Chinese and abstract in English)
- Zhang PS, Yan W, Zhang WQ, Shen BT, Wang H (2016) Mechanism of water inrush due to damage of floor and fault activation induced by mining coal seam with fault defects under fluid-solid coupling mode. *Chin J Geotechn Eng* 38:877–889 (in Chinese and abstract in English)
- Zhu WC, Wei CH (2011) Numerical simulation on mining-induced water inrushes related to geologic structures using a damage-based hydromechanical model. *Environ Earth Sci* 62:43–54
- Zhu QH, Feng MM, Mao XB (2008a) Numerical analysis of water inrush from working-face floor during mining. *J Chin Univ Min Technol* 18:159–163
- Zhu SY, Jiang ZQ, Hou HL, Xiao WG, Yao P (2008b) Analytical model and application of stress distribution on mining coal floor. *J Chin Univ Min Technol* 18:13–17